


Disruption of Synaptic Transmission in the Bed Nucleus of the Stria Terminalis Reduces Seizure-Induced Death in DBA/1 Mice and Alters Brainstem E/I Balance

ASN Neuro
Volume 14: 1–16
© The Author(s) 2022
Article reuse guidelines:
sagepub.com/journals-permissions
DOI: 10.1177/17590914221103188
journals.sagepub.com/home/asn



Maya Xia*, Benjamin Owen*, Jeremy Chiang, Alyssa Levitt, Katherine Preisinger, Wen Wei Yan, Ragan Huffman and William P. Nobis 

Abstract

Sudden unexpected death in epilepsy (SUDEP) is the leading cause of death in refractory epilepsy patients. Accumulating evidence from recent human studies and animal models suggests that seizure-related respiratory arrest may be important for initiating cardiorespiratory arrest and death. Prior evidence suggests that apnea onset can coincide with seizure spread to the amygdala and that stimulation of the amygdala can reliably induce apneas in epilepsy patients, potentially implicating amygdalar regions in seizure-related respiratory arrest and subsequent postictal hypoventilation and cardiorespiratory death. This study aimed to determine if an extended amygdalar structure, the dorsal bed nucleus of the stria terminalis (dBNST), is involved in seizure-induced respiratory arrest (S-IRA) and death using DBA/1 mice, a mouse strain which has audiogenic seizures (AGS) and a high incidence of postictal respiratory arrest and death. The presence of S-IRA significantly increased c-Fos expression in the dBNST of DBA/1 mice. Furthermore, disruption of synaptic output from the dBNST via viral-induced tetanus neurotoxin (TeNT) significantly improved survival following S-IRA in DBA/1 mice without affecting baseline breathing or hypercapnic (HCVR) and hypoxic ventilatory response (HVR). This disruption in the dBNST resulted in changes to the balance of excitatory/inhibitory (E/I) synaptic events in the downstream brainstem regions of the lateral parabrachial nucleus (PBN) and the periaqueductal gray (PAG). These findings suggest that the dBNST is a potential subcortical forebrain site necessary for the mediation of S-IRA, potentially through its outputs to brainstem respiratory regions.

Keywords

SUDEP, DBA/1, epilepsy, extended amygdala, bed nucleus of the stria terminalis

Knowledge Environments

Epilepsy<Neurodegeneration, Neurotransmission<Neurosignaling

Received January 3, 2022; Revised April 22, 2022; Accepted for publication May 5, 2022

Summary Statement

This study used a viral expression technique to disrupt synaptic output in the bed nucleus of the stria terminalis (BNST) of DBA/1 audiogenic seizure mice. Inactivating the BNST significantly improved survival following seizures and altered brainstem excitation/inhibition balance.

monitored settings reveal that onset of apnea occurs prior to cardiac dysfunction and death (Ryvlin et al., 2013), with SUDEP in rodent models following this same sequence of events (Jefferys et al., 2019; Lertwittayanon et al., 2019). This suggests that seizure-related respiratory dysfunction may play an important role in the mechanism of SUDEP.

Introduction

Sudden unexpected death in epilepsy (SUDEP) is the leading cause of death in refractory epilepsy patients (Sveinsson et al., 2017). Due to its unpredictable and largely unwitnessed nature, SUDEP is poorly understood, and its pathophysiological mechanisms remain unknown. SUDEP cases captured in

Department of Neurology, Vanderbilt University Medical Center, Nashville, TN, USA

*Denotes equal contribution.

Corresponding Author:

Department of Neurology, Vanderbilt University Medical Center, 6130A MRB 3/Bio Sci Building, 465 21st Ave S, Nashville, TN 37235, USA.
Email: william.p.nobis@vumc.org



Recent human studies have shown that stimulation of the amygdala can induce apneas, and onset of apnea is closely related to seizure spread to the amygdala (Dlouhy et al., 2015; Lacuey et al., 2017; Nobis et al., 2018, 2019; Rhone et al., 2020). In particular, stimulation of certain portions of amygdala subnuclei may be more likely to produce apneas, with the lateral and basal areas not involved in apnea production (Nobis et al., 2018; Rhone et al., 2020). This implicates amygdalar regions associated with the extended amygdala complex, which is made up in part of the bed nucleus of the stria terminalis (BNST) and the medial and central amygdala (CeA). Because extended amygdala regions have dense reciprocal connections to brainstem respiratory, autonomic, and arousal-related nuclei, these areas are strong candidates to be involved in the neural circuit underlying seizure-related apneas.

Prior studies have shown that lesioning of the CeA in mouse models of SUDEP, including DBA/1 and Dravet Syndrome mice, can increase survival following seizures and reduce the risk of apnea during seizures (Marincovich et al., 2019; Bravo et al., 2021). The BNST, a complex and heterogeneous structure composed of at least 18 subdivisions, is highly interconnected to the CeA (Gungor et al., 2015; Lebow & Chen, 2016; Partridge et al., 2016; Luskin et al., 2021; Hammack et al., 2021). More specifically, the dorsal BNST (dBNST), which is part of the anterior BNST located dorsal to the anterior commissure, has dense projections to respiratory-related nuclei, including the parabrachial nucleus (PBN), periaqueductal gray (PAG), ventral-lateral portion of the medulla (VLM), nucleus tractus solitarius (NTS), and serotonergic neurons in the dorsal and midbrain raphe nuclei (Dong & Swanson, 2004, 2006; Pollak Dorocic et al., 2014; Torruella-Suárez & McElligott, 2020; Luskin et al., 2021). This suggests that the dBNST may be another critical region involved in respiratory dysfunction during seizures.

Importantly, optogenetic stimulation of the dBNST decreases respiratory rate (Kim et al., 2013), further supporting that this subcortical region may play an important role in modulating respiration. The BNST has outputs to brainstem regions that are not only involved in modulating respiratory rate, but also involved in the response to continued respiratory dysfunction following seizures such as hypercapnic response which is mediated in part by the PBN and dorsal raphe (Bowman et al., 2013; Kaur et al., 2013; Damasceno et al., 2014). dBNST neurons, especially those projecting to the respiratory-related PBN, also express changes in excitability in a Dravet Syndrome mouse model, which has an increased incidence of sudden death (Yan et al., 2021). The BNST also has outputs to other areas that could potentially be implicated in central respiratory dysfunction such as the oxygen conserving reflexes including the diving reflex mediated in part by the NTS, which is highly interconnected to the BNST (Panneton et al., 2012; Biggs et al., 2021). Monosynaptic projections from the BNST also exist that may contribute to obstructive apneas that further complicate seizure-related respiratory dysfunction with connections to the hypoglossal nucleus and the

dorsal motor nucleus of the vagus (Dong & Swanson, 2003; Guo et al., 2020). Altogether, these findings suggest that the dBNST may play an important role in seizure-related respiratory dysfunction and death.

In this study, we aimed to determine whether the dBNST is involved in seizure-induced respiratory arrest (S-IRA) in the DBA/1 mouse model of SUDEP. DBA/1 mice have audiogenic seizures (AGS) when exposed to a loud broad tone, and these seizures are followed by a very high incidence of S-IRA, cardiac arrest, and sudden death (Faingold et al., 2010; Kommajosyula et al., 2017; Zhang et al., 2018; Kommajosyula & Faingold, 2019; Marincovich et al., 2019; Schilling et al., 2019), making DBA/1 mice a reliable model of SUDEP.

To study the role of the dBNST in S-IRA, we first analyzed neuronal activation of the dBNST following S-IRA through immunohistochemical methods. We then used a viral-mediated strategy to disrupt synaptic transmission in the dBNST to promote survival following seizures in these mice. Finally, we examined whether lesioning of the dBNST affected breathing, chemoreception, or excitatory-inhibitory balance in brainstem regions.

Methods

Mouse Husbandry and Genotyping

All experiments conducted with live mice were reviewed and approved by the Vanderbilt University Institutional Animal Care and Use Committee. Animal care and experimental procedures were carried out in accordance with the National Institutes of Health Guide for the Care and Use of Laboratory Animals. DBA/1 mice were obtained from The Jackson Laboratory (Bar Harbor, ME) and Envigo (Indianapolis, IN) and group-housed under standard laboratory conditions (14 h light/10 h dark) in the mouse facility. Mice were provided food and water ad libitum.

Priming for Audiogenic Seizures

DBA/1 mice (P25–28) were primed to have AGS in a manner consistent with the extant literature on this strain (Venit et al., 2004; Faingold et al., 2010; Zhang et al., 2017; Marincovich et al., 2019; Schilling et al., 2019). Mice were exposed to a broad tone at 90–100 dB using an alarm bell (Floyd Bell, Columbus, OH) once daily for 1 min. With the continued sound stimulation, animals either have no response (NR) or sudden onset of running behavior (wild-running seizure), and the wild run can progress into a clonic-tonic (convulsive) seizure where the animal will fall and kick its limbs violently followed by a tonic phase with rigid extension of the hindlimbs. Following the tonic phase of a seizure, there is respiratory arrest signaled by both relaxation of the pinnae and gasping which, in prior studies (Faingold et al., 2010), invariably signifies respiratory arrest and imminent death if the animal is not ventilated. Seizures were assessed by eye and

recorded as either NR, wild-running seizure (WR), or convulsive (TC) seizure in this manner, with those animals experiencing a convulsive seizure being ventilated with a manual ventilator to prevent death, as shown to be successful in prior literature (Venit et al., 2004; Faingold et al., 2010; Feng & Faingold, 2015). Priming was continued until mice had full convulsive seizures with respiratory arrest for a minimum of three days or until mice were primed for a full week (7 days). Fully primed mice were used in experiments. Three weeks following the viral injection, mice (P50-80) were retested to evaluate survival following S-IRA and used for whole-body plethysmography and electrophysiology. Mice that did not have 3 seizures were not included in the survival study.

c-Fos Fluorescent Immunohistochemistry

After DBA/1 mice were primed for a week, mice that did not exhibit 3 seizures were exposed to the audio tone again the next day, and the response was recorded as a clonic-tonic seizure with respiratory arrest, wild-running seizure, or NR. Mice were then transcardially perfused with 4% PFA 90 min after audio exposure. Perfusion and immunohistochemistry were conducted as previously described in Yan et al., 2021 to stain for *c-Fos* (Abcam).

Stereotaxic Surgeries and Viral Vectors

DBA/1 mice that were fully primed for seizures were anesthetized using isoflurane (initial dose: 3%; maintenance dose: 1.5%) and injected intracranially with AAV-DJ-CMV-eGFP-2A-TeNT or AAV-DJ-CMV-hrGFP (Stanford Neuroscience Gene Vector and Virus Core, Palo Alto, CA). Targeted microinjections were made bilaterally into the dBNST (coordinates from Bregma, medial/lateral: ± 1.18 mm, anterior/posterior: 0.18 mm, dorsal/ventral: -4.0 mm). Mice were treated with the analgesic Meloxicam (Patterson Veterinary Supply, Dallas, TX) for 48 h following surgery to reduce postoperative pain.

The AAV-DJ subtype is an AAV-2, -8, and -9 chimera created to maximize efficiency of infection in mammalian cells (Grimm et al., 2008), while the cytomegalovirus (CMV) promoter primarily ensures neuronal protein transduction (Lawlor et al., 2009; Yaguchi et al., 2013). Tetanus neurotoxin (TeNT) blocks Ca^{2+} -evoked synaptic vesicle fusion and transmitter release by cleaving VAMP2 (also known as synaptobrevin-2) (Schiavo et al., 1992; Schoch et al., 2001; Yamamoto et al., 2003). Cleavage results in improper SNARE complex formation for synaptic vesicles, while leaving other forms of vesicular fusion intact. This strategy and virus is effective in silencing synaptic output from target neurons (Li et al., 2019; Zingg et al., 2020).

Whole-Body Plethysmography

Whole-body plethysmography chambers (DSI, Harvard Biosciences, Inc.) were used to capture breathing changes

during S-IRA in bilaterally injected mice in a subset of animals. Three weeks after stereotaxic injections, mice were placed into a plethysmography chamber and exposed to a loud broad tone to induce AGS. Traces were plotted in Graphpad Prism. Seizure onset in the plethysmography trace was determined based on the trace itself.

Whole-body plethysmography was also used to evaluate changes in baseline breathing and in hypoxic and hypercapnic conditions three weeks post-injection. On the first day of trials, mice were acclimated in the plethysmography chambers for 50 min. Approximately 24 h later, baseline breathing was recorded for 50 min. On the third day, baseline breathing was recorded for 30 min, then hypercapnia (5% CO_2) was induced for 8 min followed by a 5 min washout period. On the final day, following a 30 min baseline recording, hypoxia (8% O_2) was induced for 8 min with a 5 min washout period after. Respiratory data (minute ventilation, breaths per minute, tidal volume) was analyzed using the DSI software and a custom-written Python script.

Verification of Injection Location

Animals that survived the audiogenic-induced seizure were deeply anesthetized and transcardially perfused with ice-cold PBS followed by 4% PFA. For animals that did not survive the seizure, the brain was removed and fixed in 4% PFA. For animals used in electrophysiology, the brain was removed, and the brainstem was sliced for recording. The remainder of the brain was placed in 4% PFA overnight for fixation.

Brains were coronally sectioned (30 μm) using a vibratome (Leica Biosystems, Wetzlar, Germany) and slices containing the BNST were mounted on microscope slides. Slides were then visualized on a Leica DFC290 microscope (Leica Biosystems, Wetzlar, Germany) to verify the viral expression. SigmaPlot was used to generate a heat map showing viral expression of the AAV-TeNT virus in bilaterally injected mice that survived.

Acute Slice Preparation

Acute brain slices were prepared from DBA/1 mice 3–8 weeks following stereotaxic injection of AAV-DJ-CMV-eGFP-2A-TeNT or AAV-DJ-CMV-hrGFP. Animals of both sexes were used in accordance with Institutional Animal Care and Use Committee-approved protocols. Slices were prepared as previously described (Yan et al., 2021).

Briefly, mice were anesthetized under isoflurane and decapitated. The brain was removed and coronal slices (200–250 μm) containing either the PBN or the PAG were sectioned on a vibratome (Leica VT1200S, Wetzlar, Germany) in ice-cold oxygenated sucrose solution (in mM): 85 NaCl, 2.5 KCl, 1.25 NaH_2PO_4 , 25 $NaHCO_3$, 25 glucose, 75 sucrose, 0.5 sodium ascorbate, 0.1 kynurenic acid, 0.01 DL-APV, 0.5 $CaCl_2$, 4.0 $MgCl_2$, pH 7.39–7.42, bubbled with 95% O_2 /5% CO_2 . Slices were kept in oxygenated sucrose solution in a holding chamber at 37°C and bubbled with 95% O_2 /5% CO_2

for at least 30 min. Slices were then transferred to a holding chamber containing oxygenated artificial cerebrospinal fluid (ACSF) at room temperature containing (in mM) 125 NaCl, 2.4 KCl, 1.2 NaH₂PO₄, NaHCO₃, 25 glucose, pH 7.39–7.41 bubbled with 95% O₂/5% CO₂ and maintained under these conditions until transferred to a submerged recording chamber for recording.

Electrophysiological Recordings

Slices were perfused with oxygenated ACSF at 2.0 ml/min and maintained at 34°C. Lateral PAG (IPAG) and lateral PBN (IPBN) neurons were identified using differential interference contrast on a Slicescope II microscope (Scientifica) and whole-cell patch-clamp recordings performed using borosilicate glass micropipettes (2–8 MΩ). Signals were acquired using an Axon Multiclamp 700B amplifier (Molecular Devices) and the data was sampled at 10 kHz with a gain of 1 and a Bessel low-pass filter of 3 or 10 kHz. Series resistance was uncompensated. Access resistances were continuously monitored at 3–18 MΩ and changes >20% from the initial value were excluded from data analyses. Data were collected and analyzed using Clampex 11.1 (Molecular Devices).

Voltage clamp was performed using a cesium-methanesulfonate intracellular solution containing (in mM) 135 Cs-methanesulfonate, 10 KCl, 1 MgCl₂, 20 sodium-phosphocreatine, 5.0 QX-314, 0.2 EGTA, 4.0 Mg-ATP, 0.3 Na-ATP, pH. 7.3, 290 mOsm. Upon break-in, cells were held at a membrane potential of –70 mV for at least 2 min to check for cell health and seal stability before recording the access resistance. For spontaneous excitatory postsynaptic currents (sEPSCs), cells were held at a membrane potential of –70 mV and signals recorded for 1–2 min. Following this, cells were slowly ramped to a membrane potential of +10 mV and spontaneous inhibitory postsynaptic currents (sIPSCs) recorded for 1–2 min. At the end of the recording, cells were ramped to a membrane potential of –70 mV and access resistance re-measured. Cells that experienced a change in access resistance of more than 20%, had fewer than 100 events during recording, or were unstable before both sEPSCs and sIPSCs were recorded, were disqualified from analysis. This internal solution and method for isolating inhibitory and excitatory events is consistent with methods used in other studies in the literature (Kim et al., 2013; Masneuf et al., 2014; Hwa et al., 2019; Bartsch et al., 2020; Yan et al., 2021).

Experimental Design and Statistical Analysis

Number of animals used and number of cells evaluated for each experiment are included in the Results section. Mean ± SEM values are included throughout the text. Graphical data is depicted with mean and SEM. Outliers are noted in the text and were removed if values were outside the 95% confidence interval.

Only animals injected with the AAV-DJ-CMV-eGFP-2A-TeNT virus with accurate bilateral targeting of the dBNST and appreciable expression of the virus were included; animals with unilateral targeting, lack of any appreciable fluorescence in the dBNST, or inaccurate targeting of the dBNST were excluded from analysis.

For the electrophysiology data, sEPSCs and sIPSCs were analyzed using MiniAnalysis (Synaptosoft). Signals at least twice the root-mean square of the noise were analyzed for amplitude and inter-event interval. Cumulative probability plots of sEPSC and sIPSC amplitudes and inter-event intervals (IEIs) were generated from binning all the data (IPBN: excitatory events- 1885 GFP control and 3734 TeNT, inhibitory events- 2010 GFP control and 4137 TeNT; IPAG: excitatory events- 2004 GFP control and 5129 TeNT, inhibitory events- 775 GFP control and 2359 TeNT) and compared using the Kolmogorov-Smirnov (K-S) test. For these distributions, results were considered different using a conservative critical probability of $p < 0.001$. Mean sEPSC and sIPSC amplitude and frequency were calculated and compared using Mann-Whitney test. A p -value of ≤ 0.05 was considered statistically significant.

Results

c-Fos Expression in the dBNST Significantly Increases Following S-IRA

To investigate how S-IRA affects dBNST neuronal activation, we induced AGS in DBA/1 mice and quantified the number of cells expressing the immediate early gene *c-Fos* (Figure 1A). Mice had one of three responses following audiogenic priming: NR, wild-running (WR), or clonic-tonic (TC) seizure with S-IRA (followed by resuscitation). Immunohistochemistry staining revealed that animals responding with TC seizures had significantly more *c-Fos* positive cells in the dBNST compared to animals responding with WR seizures or NR (NR: 398.5 ± 42.3 cells/mm², $n = 8$; WR: 387.9 ± 33.1 cells/mm², $n = 9$; TC: 864.5 ± 70.8 cells/mm², $n = 14$; NR vs. TC: $p = 0.0001$; WR vs. TC: $p < 0.0001$; Figure 1B, C). We found no difference in *c-Fos* expression between animals with WR and NR (NR vs. WR: $p = 0.84$; Figure 1B, C), suggesting that the significant increase in activation may result from a seizure followed by respiratory arrest.

In addition to the dBNST, the CeA was stained for *c-Fos* expression since previous studies show that electrolytic lesioning of this area can significantly increase survival after S-IRA (Marincovich et al., 2019). However, we found little expression in all conditions (Figure 1C). We also looked at *c-Fos* expression in the PAG, which has been shown to have increased activity after S-IRA in DBA/1 mice (Kommajosyula et al., 2017), and we found greater expression in mice with S-IRA, consistent with reports in the literature (Figure 1C). Finally, the inferior colliculus was stained as a positive control since this brain region is part of the auditory pathway and, as previously reported, shows consistent *c-Fos* expression with all

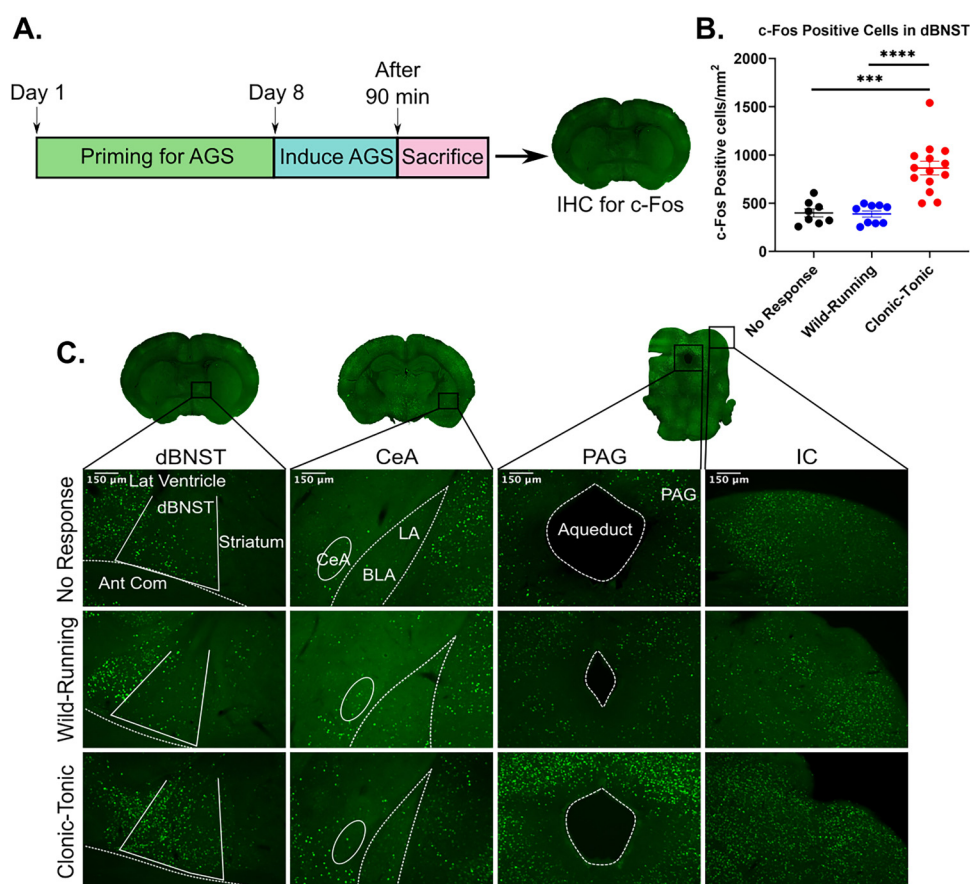


Figure 1. dBNST c-Fos expression significantly increases following seizure-induced respiratory arrest. **A.** Schematic showing timeline for priming DBA/1 mice for seizures. On day 8, animals were primed resulting in no response (NR), wild-running (WR), or clonic-tonic seizure with S-IRA (TC), followed by immunohistochemistry for c-Fos in dBNST of mice. **B.** Scatter plot depicting significant differences in c-Fos positive cells/mm² in dBNST sections for NR vs TC and WR vs TC (NR: n = 8; WR: n = 9; TC: n = 14; NR vs TC: p = 0.0001, WR vs TC: p < 0.0001). No difference in c-Fos expression between NR and WR (p = 0.84). **C.** Coronal sections of dBNST, CeA, PAG, and IC regions. Representative images of c-Fos expression in mice with NR, WR, and TC response 1.5 h post-priming. ***p < 0.001, ****p < 0.0001.

seizure phenotypes of audiogenic response (Figure 1C). Overall, the significant increase in dBNST c-Fos expression after S-IRA suggests that this region of the extended amygdala is likely involved in S-IRA.

Disruption of Presynaptic Transmission in dBNST Neurons Reduces Death from S-IRA in DBA/1 Mice

With evidence to suggest that the dBNST may be activated in S-IRA, we next aimed to examine how disruption of presynaptic transmission in dBNST neurons would affect incidence of S-IRA and death in DBA/1 mice. We first primed the mice to have AGS by exposing them to a broad tone until being fully primed or for up to 7 consecutive days (Figure 2A). Animals were considered fully primed after having 3 convulsive seizures that required resuscitation via mechanical ventilation. We then bilaterally injected tetanus neurotoxin (AAV-DJ-CMV-eGFP-2A-TeNT) or a GFP control virus (AAV-DJ-CMV-hrGFP) into the dBNST of fully primed DBA/1 mice (Figure 2B).

Electrophysiology was used to confirm that viral-induced expression of tetanus neurotoxin (AAV-TeNT) successfully resulted in disruption of presynaptic transmission in dBNST neurons compared to the GFP control virus (AAV-GFP). sIPSC frequency was significantly reduced in cells expressing the AAV-TeNT virus compared to the AAV-GFP virus (AAV-GFP: 4.0 ± 1.1 Hz, n = 5 cells from 3 animals; AAV-TeNT: 0.9 ± 0.29 Hz, n = 8 cells from 4 animals; p = 0.006; Figure 2D). There was no significant change in sIPSC amplitude in the AAV-TeNT expressing cells (AAV-GFP: 23.6 ± 4.0 pA, n = 5 cells; AAV-TeNT: 21.9 ± 2.5 pA, n = 8 cells; p = 0.72; Figure 2E).

Three weeks following stereotaxic injection in the dBNST, we re-induced seizures in these mice to observe if there were any differences in incidence of S-IRA and survival between the AAV-TeNT and AAV-GFP control mice. We found a significant increase in survival following disruption of presynaptic transmission in the dBNST. 42.9% of AAV-TeNT virally injected mice survived while only 7.7% of AAV-GFP mice survived (AAV-GFP: n = 26; AAV-TeNT: n = 14; p = 0.014

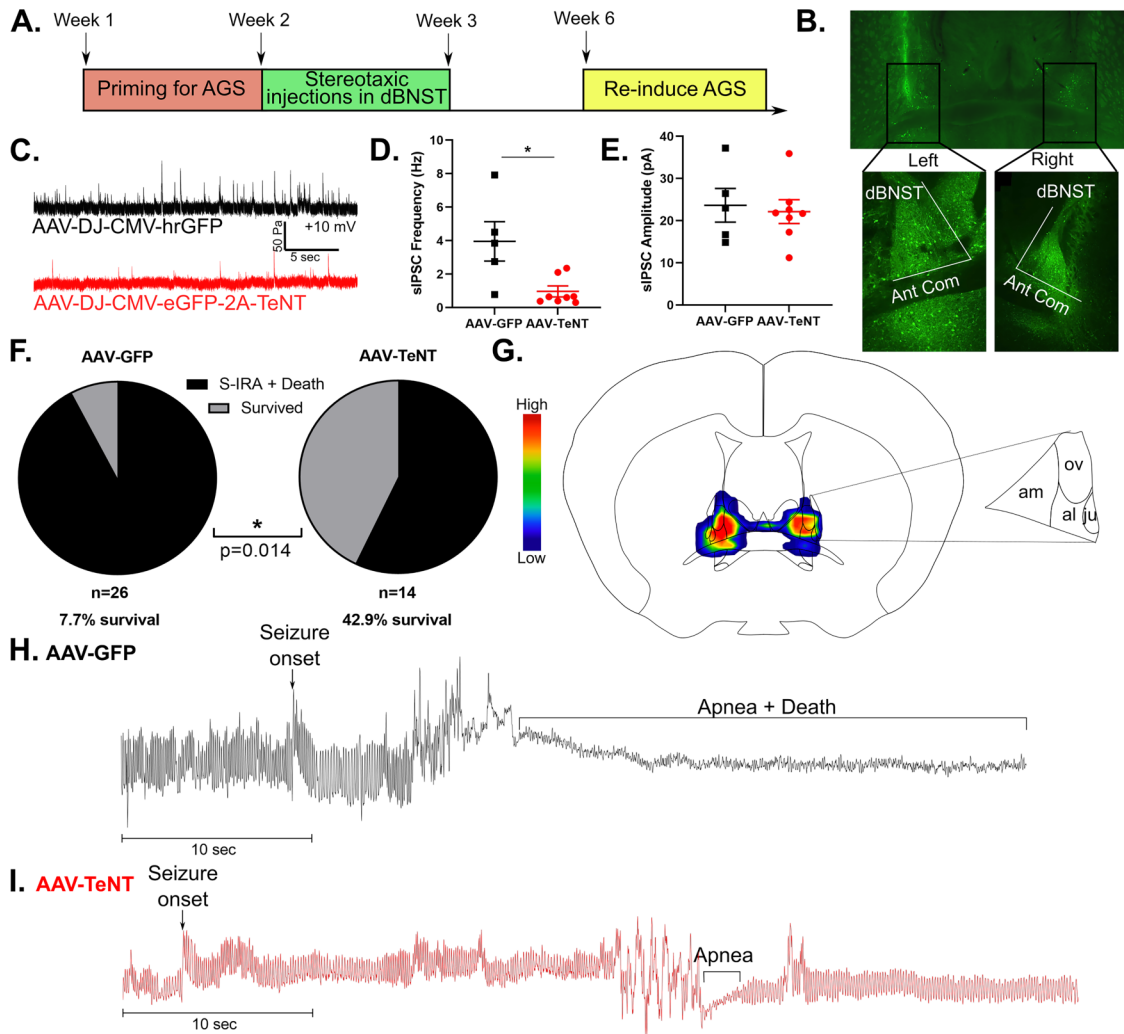


Figure 2. Disrupting presynaptic transmission in dBNST neurons reduces seizure-induced death in DBA/1 mice. **A.** Schematic showing timeline for priming DBA/1 mice for seizures, followed by stereotaxic injections and re-induction of seizures to observe survival rate. **B.** Representative image showing bilateral viral expression of AAV-DJ-CMV-eGFP-2A-TeNT in left and right dBNST. **C.** Representative trace of sIPSCs in dBNST neurons of animals with viral expression of AAV-GFP vs. AAV-TeNT. **D.** Graph shows significant reduction in sIPSC frequency in cells expressing AAV-TeNT (AAV-GFP: $n = 5$ cells from 3 animals; AAV-TeNT: $n = 8$ cells from 4 animals; $p = 0.006$). **E.** Graph showing no difference in sIPSC amplitude between AAV-GFP and AAV-TeNT expressing cells (AAV-GFP: $n = 5$ cells from 3 animals; AAV-TeNT: $n = 8$ cells from 4 animals; $p = 0.72$). **F.** Graph depicting significant increase in survival following S-IRA in AAV-TeNT virus-injected animals compared to AAV-GFP animals (AAV-GFP: $n = 26$; AAV-TeNT: $n = 14$; $p = 0.014$). **G.** Heat map on atlas image shows AAV-TeNT viral expression in dBNST for mice that survived (am: anteromedial area, ov: oval nucleus, al: anterolateral area, ju: juxtacapsular nucleus). **H.** Representative plethysmography trace in AAV-GFP animal showing S-IRA followed by death. **I.** Representative plethysmography trace in AAV-TeNT animal depicting survival following S-IRA. $*p < 0.05$.

Fisher's exact test; Figure 2F). Unilateral targeting of the dBNST was insufficient to prevent death in AAV-TeNT mice, and only 4.3% of animals with unilateral targeting survived ($n = 23$), similar to the survival rate in the AAV-GFP group. Thus, the AAV-TeNT group only consisted of animals with accurate bilateral targeting of the dBNST. In mice that survived, bilateral viral expression of AAV-TeNT was greatest in the anteromedial area of the dBNST, followed by high levels of expression in the oval nucleus and anterolateral area (Figure 2G), consistent with the localization of c-Fos expression in the dBNST after S-IRA (Figure 1C).

Using whole-body plethysmography to visualize breathing during S-IRA, we found that in AAV-GFP mice that died from S-IRA, seizures were followed by apnea and death (Figure 2H). In contrast, AAV-TeNT mice that survived experienced seizures that resulted in short apneas followed by return to normal breathing (Figure 2I).

Animals that did not have seizures three weeks following the stereotaxic injection were excluded from survival analysis. There was no relationship to the type of viral injection in those animals that were non-responders to audio tone. These animals may have lost seizure susceptibility due to the placement of ear bars during

surgery, damaging their eardrums and decreasing their ability to perceive sound and thus have an audiogenic seizure. Susceptibility to AGS changes and often diminishes as DBA/1 mice age, so age could also explain why we could not re-induce seizures in some fully primed mice (Martin et al., 2020).

Disruption of Synaptic Output in the dBNST Does not alter Breathing or Chemoreception

To determine if disrupting synaptic output of the dBNST affects breathing or chemoreception, we used whole-body plethysmography to analyze baseline breathing, hypercapnic ventilatory response (HCVR), and hypoxic ventilatory response (HVR; Figure 3A). There were no changes in baseline breathing respiratory rate (AAV-GFP: $100 \pm 5.7\%$, $n = 24$; AAV-TeNT: $104.7 \pm 9.1\%$, $n = 16$; $p = 0.65$; Figure 3B), minute ventilation (AAV-GFP: $100 \pm 7.0\%$, $n = 24$; AAV-TeNT: $101.5 \pm 8.5\%$, $n = 16$; $p = 0.89$; Figure 3C), or tidal volume (AAV-GFP: $100 \pm 7.7\%$, $n = 24$; AAV-TeNT: $96.4 \pm 8.6\%$, $n = 16$; $p = 0.76$; Figure 3D) between AAV-GFP and AAV-TeNT mice.

We found no differences between AAV-GFP and AAV-TeNT animals in HCVR respiratory rate (AAV-GFP: $122.4 \pm 7.5\%$, $n = 21$ with 3 high outliers removed; AAV-TeNT: $118.2 \pm 4.7\%$, $n = 16$; $p = 0.59$; Figure 3E) and minute ventilation (AAV-GFP: $162.9 \pm 8.9\%$, $n = 24$; AAV-TeNT: $172 \pm 8.6\%$, $n = 16$; $p = 0.49$; Figure 3F), but there was a significant increase in tidal volume (AAV-GFP: $124.7 \pm 4.7\%$, $n = 24$; AAV-TeNT: $142.4 \pm 7.2\%$, $n = 16$; $p = 0.037$; Figure 3G) of AAV-TeNT animals. Increased CO_2 can induce panic behavior in mice, and this response is dependent on BNST function (Taughner et al., 2014). Therefore, the increase in tidal volume in the AAV-TeNT animals may represent blunted panic behavior due to hypofunctioning of the BNST, with an otherwise preserved chemosensory response.

Finally, there were no significant differences in HVR respiratory rate (AAV-GFP: $124.8 \pm 8.7\%$, $n = 24$; AAV-TeNT: $106.3 \pm 5.9\%$, $n = 16$; $p = 0.12$; Figure 3H), minute ventilation (AAV-GFP: $173.7 \pm 9.0\%$, $n = 24$; AAV-TeNT: $155.5 \pm 7.8\%$, $n = 16$; $p = 0.16$; Figure 3I), or tidal volume (AAV-GFP: $138.8\% \pm 5.0\%$, $n = 24$; AAV-TeNT: $145.7 \pm 5.4\%$, $n = 16$; $p = 0.37$; Figure 3J) between AAV-GFP and AAV-TeNT mice. Overall, these results suggest that the dBNST is not involved in baseline breathing or respiration in response to chemoreception, which is consistent with previous studies (Granjeiro et al., 2012; Taughner et al., 2014).

Disrupting Presynaptic Transmission from the dBNST Neurons Altered Excitatory Synaptic Drive in the Downstream Brainstem Region of the Lateral Parabrachial Nucleus

Given the disruption in S-IRA and the BNST projections to brainstem respiratory regions, we wanted to determine if our manipulation had any effect on these end target regions

of interest. We chose to investigate the IPBN and the IPAG as they both receive dense input from the extended amygdala, are involved in respiratory control, and have been shown to be activated by S-IRA induced death in DBA/1 mice (Holstege et al., 1985; Dutschmann & Herbert, 2006; Kommajosyula et al., 2017; Faull et al., 2019; Luskin et al., 2021). To elucidate if dBNST inactivation altered E/I balance in these brainstem neurons, we recorded sEPSCs and sIPSCs in both the IPBN and IPAG neurons from GFP control ($n = 4$ animals for both IPBN and IPAG recordings) and AAV-TeNT ($n = 3$ and 5 animals for IPBN and IPAG recordings, respectively) animals.

Based on the recordings in the IPBN, we observed an increase in mean sEPSC frequency in AAV-TeNT animals compared to controls (GFP: 3.15 ± 0.25 Hz, $n = 5$ cells; TeNT: 6.23 ± 0.89 Hz, $n = 5$ cells; $p = 0.008$; Figure 4C) with a leftward shift in sEPSC IEI distribution (K-S: $p < 0.0001$; Figure 4G), indicating more frequent excitatory signaling following dBNST inactivation. We also observed a leftward shift in sEPSC amplitude distribution (K-S: $p < 0.0001$; Figure 4F), in particular a decrease in the population of larger amplitude events. However, we did not observe any significant effects of dBNST inactivation on mean sEPSC amplitude (GFP: 12.4 ± 1.4 pA, $n = 5$ cells; TeNT: 10.4 ± 0.3 pA, $n = 5$ cells; $p = 0.15$; Figure 4B). Overall, our data indicates an increase in excitatory synaptic drive in the IPBN following dBNST inactivation with a trend towards smaller excitatory synaptic events. Though we did not observe any differences in mean sIPSC amplitude (GFP: 19.4 ± 4.3 pA, $n = 5$ cells; TeNT: 27.2 ± 3.1 pA, $n = 5$ cells; $p = 0.22$; Figure 4D) or frequency (GFP: 3.4 ± 1.4 Hz, $n = 5$ cells; TeNT: 7.6 ± 1.8 Hz, $n = 5$ cells; $p = 0.09$; Figure 4E), we did observe changes in the distributions of sIPSC amplitudes and IEIs following dBNST inactivation; namely, we observed a rightward shift in the distribution of sIPSC amplitudes (K-S: $p < 0.0001$; Figure 4H) affecting smaller amplitude events, suggesting an increase in sIPSC amplitudes, and a leftward shift in the distribution of sIPSC IEIs (K-S: $p < 0.0001$; Figure 4I) similar to our observation of sEPSC IEIs, suggesting an increase in inhibitory synaptic drive.

Unlike the IPBN, the synaptic changes were more subtle in the IPAG following AAV-TeNT injections in the dBNST. Most noticeably, we observed a significant rightward shift in the distribution of sIPSC amplitudes (K-S: $p < 0.0001$; Figure 5H) with an increase in larger amplitude events and a leftward shift in the distribution of sIPSC IEIs (K-S: $p < 0.0001$; Figure 5I) but without changes in either the mean sIPSC amplitudes (GFP: 19.6 ± 2.2 pA, $n = 4$ cells; TeNT: 33.4 ± 10.6 pA, $n = 6$ cells; $p = 0.26$; Figure 5D) or the mean frequency of events (GFP: 1.6 ± 0.2 Hz, $n = 4$ cells; TeNT: 3.3 ± 0.7 Hz, $n = 6$ cells; $p = 0.17$; Figure 5E), suggesting a trend toward increased inhibitory synaptic drive in the IPAG following dBNST inactivation. Likewise, there were no differences in mean sEPSC amplitude (GFP: 16.8 ± 1.8 pA, $n = 4$ cells; TeNT: 11.8 ± 1.3 pA, $n = 6$ cells; $p = 0.07$;

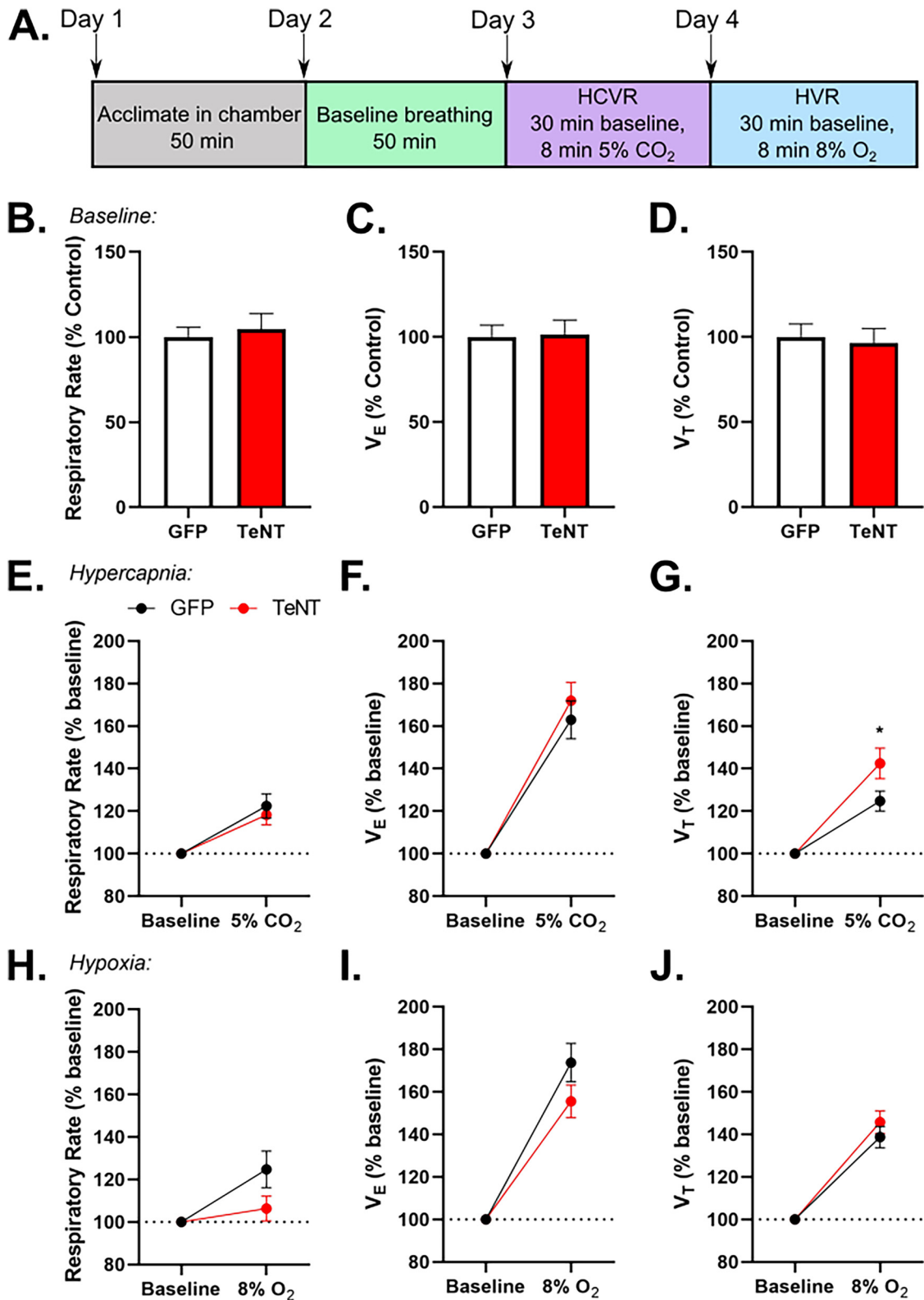


Figure 3. Disrupting synaptic output in dBNST neurons does not significantly alter breathing or chemoreception. **A.** Schematic showing experimental design for whole-body plethysmography trials. No difference in baseline breathing **B.** respiratory rate (AAV-GFP: $n = 24$; AAV-TeNT: $n = 16$; $p = 0.65$), **C.** V_E ($p = 0.89$), or **D.** V_T ($p = 0.76$) between AAV-GFP and AAV-TeNT injected animals. No difference in **E.** respiratory rate ($p = 0.59$) and **F.** V_E ($p = 0.49$). AAV-TeNT animals had a significant increase in **G.** V_T ($p = 0.037$) during hypercapnic conditions. No changes in HVR **H.** respiratory rate ($p = 0.12$), **I.** V_E ($p = 0.16$), or **J.** V_T ($p = 0.37$). * $p < 0.05$ (V_E : minute ventilation; V_T : tidal volume).

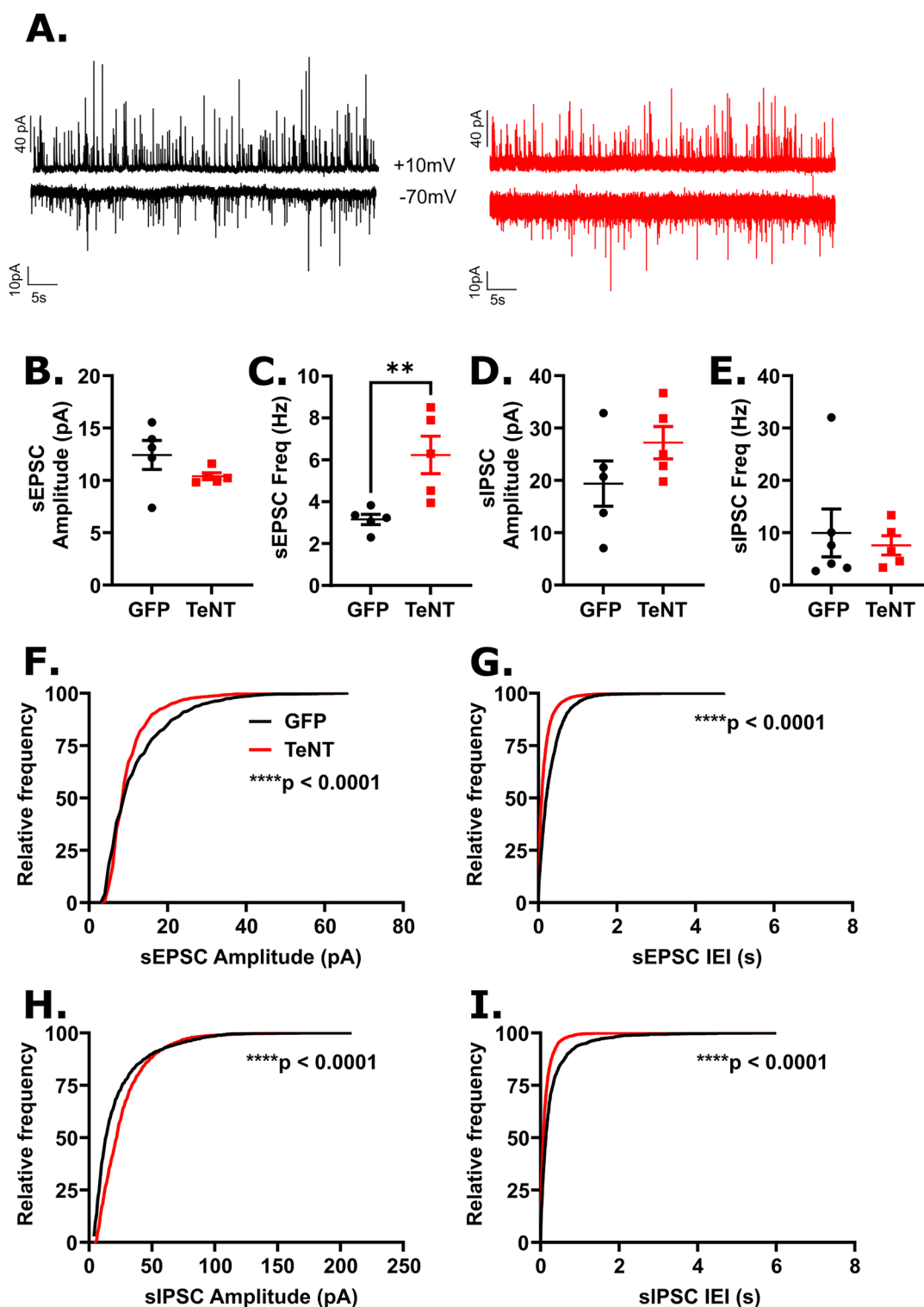


Figure 4. Disrupting synaptic output in dBNST neurons reduced excitatory synaptic drive in IPBN neurons. **A.** Examples of recordings of sEPSCs (bottom) and sIPSCs (top) recorded from GFP (black) and AAV-TeNT (red) animals ($n = 4$ and 3 animals, respectively). Each trace is 60s in duration. **B.** Mean sEPSC amplitude was not significantly affected in neurons from AAV-TeNT animals compared to control animals (GFP: $n = 5$ cells; TeNT: $n = 5$ cells; $p = 0.15$), though an increase was observed in **C.** mean frequency ($p = 0.008$). No effect of dBNST synaptic disruption was observed in **D.** mean sIPSC amplitude ($p = 0.22$) or **E.** mean frequency ($p = 0.09$). **F.** A significant leftward shift in the distribution of sEPSC amplitudes (K-S: $p < 0.0001$) was observed as was **G.** a significant leftward shift in the distribution of sEPSC frequencies (K-S: $p < 0.0001$). **H.** A significant rightward shift in the distribution of sIPSC amplitudes (K-S: $p < 0.0001$) and **I.** a significant leftward shift in the distribution sIPSC frequencies (K-S: $p < 0.0001$) were observed. ** $p < 0.01$, **** $p < 0.0001$.

Figure 5B) or frequency (GFP: 4.2 ± 0.7 Hz, $n=4$ cells; TeNT: 7.1 ± 1.4 Hz, $n=6$ cells; $p=0.17$; Figure 5C) but shifts in the distribution of sEPSC amplitudes (leftward shift; K-S: $p<0.0001$; Figure 5F) and sEPSC IEIs (leftward shift; K-S: $p<0.0001$; Figure 5G) similar to those in the IPBN were observed.

Together, our data shows that this chronic synaptic disruption of the dBNST can have effects in the downstream brainstem target regions of the IPBN and the IPAG.

Discussion

Here we demonstrated that bilateral disruption of synaptic transmission in the dBNST can greatly reduce S-IRA and death in the DBA/1 audiogenic seizure mouse model of SUDEP. Prior work elegantly demonstrated through lesion studies that the amygdala may be necessary for S-IRA in DBA/1 mice. In this study, we demonstrated that the dBNST was the extended amygdalar component that was strongly activated during seizures with respiratory arrest in DBA/1 mice as measured by expression of the immediate early gene *c-Fos*. By disrupting synaptic transmission in dBNST neurons with a viral-mediated approach, we were able to disrupt S-IRA and death in DBA/1 mice, suggesting that the dBNST is also a critical mediator of this effect. Breathing under normoxic, hypercapnic, and hypoxic conditions was not affected by these dBNST manipulations, consistent with prior findings (Granjeiro et al., 2012; Taugher et al., 2014). This suggests that the dBNST may not be involved in baseline breathing but could still play a role in mediating S-IRA and apneas. Furthermore, we investigated the influence that the relative dBNST silencing had on E/I balance in downstream brainstem respiratory regions, the IPBN and IPAG. Here we observed that we could significantly alter synaptic signaling in these regions. In general, these effects were more pronounced in the IPBN where we observed significantly increased sEPSC frequency in the TeNT group. This suggests that disruption of dBNST input to the IPBN may be disinhibiting excitatory signaling. The dBNST has both excitatory and inhibitory projections to the IPBN (Luskin et al., 2021) and also inhibitory projections to other brainstem regions that project to the PBN including the CeA and NTS (Dong & Swanson, 2003; Chiang et al., 2019), so it is not surprising that we see a complicated scenario with an increase in excitatory and a suggestion of increased inhibitory signaling following our chronic manipulation. The heterogeneous nature of the BNST combined with the relative variability in targeting of these neurons and the time allowed for compensatory changes to develop likely contribute to the overall subtle effects seen in both the IPBN and IPAG.

There is building evidence that seizure spread to, or electrical stimulation of, the amygdala can induce apneas and respiratory dysfunction in patients with epilepsy (Dlouhy et al., 2015; Nobis et al., 2018, 2019; Rhone et al., 2020). Central apneas during seizure onset have unclear clinical impact

(Tio et al., 2020), with respiratory dysfunction and apneas persisting after seizures being potentially more clinically impactful (Vilella et al., 2018). The S-IRA present in the DBA/1 mouse model consists of a rapid-onset apnea during the clonic phase of the seizure that persists with ultimate hypoventilation and death (Schilling et al., 2019). This represents a potential model for both ictal apnea and an extended postictal apnea.

Seizure-induced death in DBA/1 mice also activates brainstem regions (Kommajosyula et al., 2017). Growing evidence from chemoconvulsant seizure models suggests spread of seizures into the brainstem are associated with apneas and death (Jefferys et al., 2019; Lertwittayanon et al., 2019) and that brainstem seizures can be associated with brainstem spreading depolarization (Jansen et al., 2019). We propose that prior clinical and preclinical evidence, along with our current study, suggest that the extended amygdala is a potential node for seizure propagation to brainstem respiratory structures, producing central apneas and also impairing respiratory rescue responses and ultimately increasing the risk for SUDEP.

This study appears to stand in contrast to the work implicating the central amygdala (CeA) as necessary for S-IRA (Marincovich et al., 2019). However, given the highly connected nature of the CeA and BNST, it is not unexpected that we have similar results with manipulations to the dBNST. The clinical stimulation data clearly implicates a region in the centromedial amygdala as an area that can readily produce an apnea, but it is also apparent from preclinical studies that the BNST can have a similar function in modulating respiratory rate (Kim et al., 2013). The BNST is also involved in arousal (Kodani et al., 2017) and has projections to important chemosensory structures such as the raphe (Weissbourd et al., 2014), so its activation during seizures may be important in both initial apnea generation but also in continued respiratory and arousal deficits with seizures. The BNST and CeA then may be working in concert in a pathological way to increase SUDEP risk if either or both are activated by a seizure.

It is unclear how often the BNST is activated by seizures as it has not been regularly evaluated in prior studies, but it's striking that *c-Fos* data here mirrors previously published *c-Fos* data in a Dravet Syndrome mouse model that also has a significant rate of SUDEP (Yan et al., 2021). Seizure activation of both the CeA and BNST may be a marker of SUDEP risk but would need to be studied in more preclinical models. We did not show significant *c-Fos* expression in the CeA in the DBA/1 model with seizures, but this does not preclude its activation as a very small subregion may be all that is needed to induce apnea, as suggested by human data (Rhone et al., 2020).

Interestingly, similar to the Marincovich et al., 2019 study, we were not able to improve survival after S-IRA in 100% of our mice with dBNST manipulations, and we were only able to improve survival following S-IRA in mice with accurate

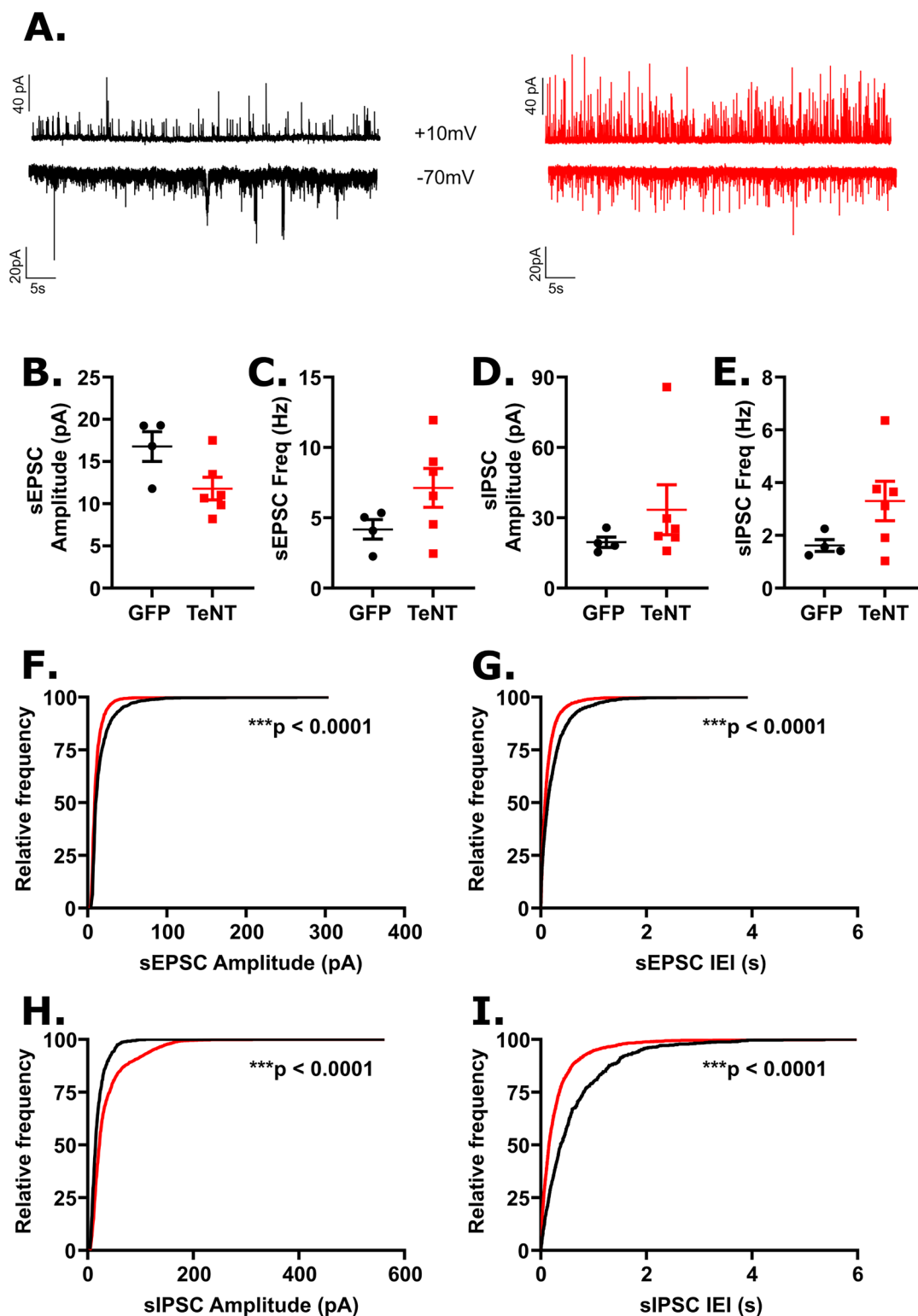


Figure 5. Disrupting dBNST synaptic output to IPAG neurons resulted in subtle changes to excitatory and inhibitory signaling. **A.** Examples of recordings of sEPSCs (bottom) and sIPSCs (top) recorded from GFP (black) and AAV-TeNT (red) animals ($n=4$ and 5 animals, respectively). Each trace is $60s$ in duration. No effect of dBNST synaptic disruption was observed in **B.** mean sEPSC amplitude (GFP: $n=4$ cells; TeNT: $n=6$ cells; $p=0.07$), **C.** mean sEPSC frequency ($p=0.17$), **D.** mean sIPSC amplitude ($p=0.26$), or **E.** mean sIPSC frequency ($p=0.17$). **F.** A leftward shift in the distribution of sEPSC amplitudes (K-S: $p < 0.0001$) and **G.** a rightward shift in the distribution of sIPSC frequencies (K-S: $p < 0.0001$) were observed. **H.** A significant rightward shift in the distribution of sIPSC amplitudes (K-S: $p < 0.0001$) and **I.** a significant leftward shift in the distribution of sIPSC frequencies (K-S: $p < 0.0001$) were observed. $***p < 0.0001$.

bilateral viral targeting of the dBNST. These findings can be attributed to several factors. First, there is likely not complete viral penetration of the dBNST since the virus may not transduce into all cells of this region. The viral-mediated approach also diminishes synaptic activity rather than lesioning the dBNST, providing greater accuracy in targeted regions while causing a response that may only be exhibited with bilateral inactivation. Additionally, the BNST is a highly heterogeneous brain region; however, our approach targets the whole dBNST rather than particular subregions or projection neurons, creating variability in survival due to differences in viral expression between animals. Moreover, since the BNST and CeA are highly interconnected, both amygdalar regions may be involved in S-IRA, and targeting cells in the BNST interconnected with the CeA may be necessary for improving survival, which could explain why there is not complete survival in both this study and the Marincovich et al., 2019 study. Hence, a multifactorial pathology likely underlies this phenomenon and makes it challenging to prevent death by inactivating just one extended amygdala region, further implicating both the BNST and CeA as potentially important regions to target in reducing SUDEP risk.

We further began to determine which brainstem region(s) the extended amygdala is acting on to influence respiratory status. The Kölliker-Fuse nucleus of the lateral PBN and the PAG are both activated during S-IRA and also activated when S-IRA is alleviated through the actions of fluoxetine (Kommajosyula et al., 2017; Kommajosyula & Faingold, 2019), making them likely candidate regions. We found virally-mediated inhibition of the dBNST altered E/I balance in both the IPBN and the IPAG to some degree with more pronounced alterations in the IPBN, exhibiting increased excitatory synaptic drive with more frequent excitatory events. Because GABAergic inhibitory signaling is a major component of dBNST signaling to other brain regions (Kim & Kim, 2021), inactivation of this nucleus could lead to disinhibition of excitatory drive from other inputs into the IPBN, allowing for an increase in survivability. That a trend toward increased inhibitory signaling was observed as well may suggest an overall disinhibition of other projections to the IPBN. Yan et al., 2021 previously found that BNST-PBN neurons in a mouse model of Dravet Syndrome and SUDEP were less likely to fire action potentials in response to current injections, building evidence on the potential importance of this pathway and risk for SUDEP. In Sudden Infant Death Syndrome (SIDS), another cause of sudden death due to respiratory dysfunction, and in Rett Syndrome, a neurodevelopmental disorder with significant apneas, the Kölliker-Fuse/lateral PBN have also been implicated (Abdala et al., 2016; Lavezzi et al., 2019; Varga et al., 2020). More broadly, stimulation of BNST-PBN projection neurons has also been shown to decrease respiratory rate (Kim et al., 2013).

Within BNST to brainstem region circuits, our BNST manipulations may also be affecting serotonergic signaling. Augmentation of serotonin (5-HT) function in DBA/1 mice promotes survival and diminishes S-IRA (Zeng et al., 2015; Faingold et al., 2016; Zhang et al., 2018). DBA/1 mice have defective expression of serotonergic receptors in the brainstem (Feng & Faingold, 2015), which may explain the ability of 5-HT augmentation in promoting survival. However, given significant extended amygdala output to dorsal raphe neurons (Weissbourd et al., 2014) and the ability of activation of BNST neurons to modulate 5-HT metabolism in the DR (Donner et al., 2019), it is possible that the extended amygdala also has a role in 5-HT dysfunction in these animals. More recently, adrenergic $\alpha 2$ receptor agonists have been shown to alleviate S-IRA in DBA/1 mice (Feng & Faingold, 2015; Zhang et al., 2021). Activation of these receptors in the BNST can modulate PBN input (Fetterly et al., 2018; Harris et al., 2018), which may provide a mechanism outside the noradrenergic role in arousal for the effect of adrenergic $\alpha 2$ receptor agonists.

This study further supports that a central apnea is critically important in leading to SUDEP, supporting human studies and observations (Ryvlin et al., 2013; Johnson et al., 2021). Overall, this study builds on the growing evidence for the extended amygdala as a key node that critically affects respiratory function and apnea induction but potentially has multiple levels of influence in SUDEP pathophysiology. More studies will be needed to fully test this hypothesis, in particular to begin to address the heterogeneity of this region and determine those neuronal populations that are most critically involved in S-IRA. Determination of these precise neuronal populations will aid in development of therapeutic targets to prevent death in SUDEP and other syndromic sudden death entities including SIDS, whether through neuromodulation of these extended amygdalar pathways or neuromodulation of other brain regions that may counteract the respiratory and arousal depression. More broadly, this study further defines the extended amygdala as a higher order structure that can modulate brainstem respiratory networks.

In summary, we demonstrated that a bilateral virally-mediated impairment in dBNST synaptic function greatly diminished S-IRA and altered E/I balance in brainstem respiratory regions, suggesting that the BNST may represent an important node in the pathway by which seizures spread to the brainstem to cause death in the DBA/1 audiogenic seizure model of SUDEP.

Acknowledgments

The authors would like to acknowledge Cierra Lyons, Emily Miller and Merium Easterling for assistance in experiments, and Jagath Vytheswaran for writing Python scripts for plethysmography analysis.

Declaration of Conflicting Interests

The author(s) declared no potential conflicts of interest with respect to the research, authorship, and/or publication of this article.

Funding

The author(s) disclosed receipt of the following financial support for the research, authorship, and/or publication of this article: This work was supported by the American Epilepsy Society (Junior Investigator Award), Vanderbilt University (Vanderbilt Faculty Research Scholars (VFRS) Award), the National Center for Advancing Translational Sciences (grant number KL2TRO02245), and the National Institute of Neurological Disorders and Stroke (Center for SUDEP Research (CSR)).

ORCID iD

William P. Nobis  <https://orcid.org/0000-0002-2318-6077>

References

- Abdala, A. P., Toward, M. A., Dutschmann, M., Bissonnette, J. M., & Paton, J. F. R. (2016). Deficiency of GABAergic synaptic inhibition in the Kölliker-Fuse area underlies respiratory dysrhythmia in a mouse model of Rett syndrome. *The Journal of Physiology*, *594*(1), 223–237. <https://doi.org/10.1113/JP270966>
- Bartsch, J. C., Jamil, S., Remmes, J., Verma, D., & Pape, H.-C. (2020). Functional deletion of neuropeptide Y receptors type 2 in local synaptic networks of anteroventral BNST facilitates recall and increases return of fear. *Molecular Psychiatry*, *26*, 2900–2911. <https://doi.org/10.1038/s41380-020-0846-x>
- Biggs, E. N., Budde, R., Jefferys, J. G. R., & Irazoqui, P. P. (2021). Ictal activation of oxygen-conserving reflexes as a mechanism for sudden death in epilepsy. *Epilepsia*, *62*(3), 752–764. <https://doi.org/10.1111/epi.16831>
- Bowman, B. R., Kumar, N. N., Hassan, S. F., McMullan, S., & Goodchild, A. K. (2013). Brain sources of inhibitory input to the rat rostral ventrolateral medulla. *Journal of Comparative Neurology*, *521*(1), 213–232. <https://doi.org/10.1002/cne.23175>
- Bravo, E., Teran, F., Crofts, M., Dlouhy, B., & Richerson, G. (2021). Limbic system involvement in modulation of breathing during seizures and arousal. *The FASEB Journal*, *35*(S1). <https://doi.org/10.1096/fasebj.2021.35.S1.04315>
- Chiang, M. C., Bowen, A., Schier, L. A., Tupone, D., Uddin, O., & Heinricher, M. M. (2019). Parabrachial Complex: A hub for pain and aversion. *The Journal of Neuroscience*, *39*(42), 8225–8230. <https://doi.org/10.1523/JNEUROSCI.1162-19.2019>
- Damasceno, R. S., Takakura, A. C., & Moreira, T. S. (2014). Regulation of the chemosensory control of breathing by Kölliker-Fuse neurons. *American Journal of Physiology-Regulatory, Integrative and Comparative Physiology*, *307*(1), R57–R67. <https://doi.org/10.1152/ajpregu.00024.2014>
- Dlouhy, B. J., Gehlbach, B. K., Kreple, C. J., Kawasaki, H., Oya, H., Buzza, C., Granner, M. A., Welsh, M. J., Howard, M. A., Wemmie, J. A., & Richerson, G. B. (2015). Breathing inhibited when seizures spread to the amygdala and upon amygdala stimulation. *Journal of Neuroscience*, *35*(28), 10281–10289. <https://doi.org/10.1523/JNEUROSCI.0888-15.2015>
- Dong, H.-W., & Swanson, L. W. (2003). Projections from the rhomboid nucleus of the bed nuclei of the stria terminalis: Implications for cerebral hemisphere regulation of ingestive behaviors. *The Journal of Comparative Neurology*, *463*(4), 434–472. <https://doi.org/10.1002/cne.10758>
- Dong, H.-W., & Swanson, L. W. (2004). Organization of axonal projections from the anterolateral area of the bed nuclei of the stria terminalis. *The Journal of Comparative Neurology*, *468*(2), 277–298. <https://doi.org/10.1002/cne.10949>
- Dong, H.-W., & Swanson, L. W. (2006). Projections from bed nuclei of the stria terminalis, anteromedial area: Cerebral hemisphere integration of neuroendocrine, autonomic, and behavioral aspects of energy balance. *The Journal of Comparative Neurology*, *494*(1), 142–178. <https://doi.org/10.1002/cne.20788>
- Donner, N. C., Mani, S., Fitz, S. D., Kienzle, D. M., Shekhar, A., & Lowry, C. A. (2019). Crh receptor priming in the bed nucleus of the stria terminalis induces tph2 gene expression in the dorsomedial dorsal raphe nucleus and chronic anxiety. *Progress in Neuro-Psychopharmacology & Biological Psychiatry*, *96*, 109730. <https://doi.org/10.1016/j.pnpb.2019.109730>
- Dutschmann, M., & Herbert, H. (2006). The Kölliker-Fuse nucleus gates the postinspiratory phase of the respiratory cycle to control inspiratory off-switch and upper airway resistance in rat. *European Journal of Neuroscience*, *24*(4), 1071–1084. <https://doi.org/10.1111/j.1460-9568.2006.04981.x>
- Faingold, C. L., Randall, M., & Tupal, S. (2010). DBA/1 mice exhibit chronic susceptibility to audiogenic seizures followed by sudden death associated with respiratory arrest. *Epilepsy & Behavior*, *17*(4), 436–440. <https://doi.org/10.1016/j.yebeh.2010.02.007>
- Faingold, C. L., Randall, M., Zeng, C., Peng, S., Long, X., & Feng, H.-J. (2016). Serotonergic agents act on 5-HT₃ receptors in the brain to block seizure-induced respiratory arrest in the DBA/1 mouse model of SUDEP. *Epilepsy & Behavior*, *64*(Pt A), 166–170. <https://doi.org/10.1016/j.yebeh.2016.09.034>
- Faull, O. K., Subramanian, H. H., Ezra, M., & Pattinson, K. T. S. (2019). The midbrain periaqueductal gray as an integrative and interoceptive neural structure for breathing. *Neuroscience & Biobehavioral Reviews*, *98*, 135–144. <https://doi.org/10.1016/j.neubiorev.2018.12.020>
- Feng, H.-J., & Faingold, C. L. (2015). Abnormalities of serotonergic neurotransmission in animal models of SUDEP. *Epilepsy & Behavior*, *71*(Pt B), 174–180. <https://doi.org/10.1016/j.yebeh.2015.06.008>
- Fetterly, T. L., Basu, A., Nabit, B. P., Awad, E., Williford, K. M., Centanni, S. W., Matthews, R. T., Silberman, Y., & Winder, D. G. (2018). α 2A-adrenergic receptor activation decreases parabrachial nucleus excitatory drive onto BNST CRF neurons and reduces their activity in vivo. *The Journal of Neuroscience*, *39*(3), 472–484. <https://doi.org/10.1523/JNEUROSCI.1035-18.2018>
- Granjeiro, E. M., Gomes, F. V., Alves, F. H. F., Crestani, C. C., Corrêa, F. M. A., & Resstel, L. B. M. (2012). Bed nucleus of the stria terminalis and the cardiovascular responses to chemoreflex activation. *Autonomic Neuroscience*, *167*(1-2), 21–26. <https://doi.org/10.1016/j.autneu.2011.11.004>
- Grimm, D., Lee, J. S., Wang, L., Desai, T., Akache, B., Storm, T. A., & Kay, M. A. (2008). In vitro and in vivo gene therapy vector evolution via multispecies interbreeding and retargeting of adeno-associated viruses. *Journal of Virology*, *82*(12), 5887–5911. <https://doi.org/10.1128/JVI.00254-08>
- Gungor, N. Z., Yamamoto, R., & Pare, D. (2015). Optogenetic study of the projections from the bed nucleus of the stria terminalis to the

- central amygdala. *Journal of Neurophysiology*, 114(5), 2903–2911. <https://doi.org/10.1152/jn.00677.2015>
- Guo, H., Yuan, X.-S., Zhou, J.-C., Chen, H., Li, S.-Q., Qu, W.-M., & Huang, Z.-L. (2020). Whole-brain monosynaptic inputs to hypoglossal motor neurons in mice. *Neuroscience Bulletin*, 36(6), 585–597. <https://doi.org/10.1007/s12264-020-00468-9>.
- Hammack, S. E., Braas, K. M., & May, V. (2021). Chapter 26 - Chemoarchitecture of the bed nucleus of the stria terminalis: Neurophenotypic diversity and function. In D. F. Swaab, F. Kreier, P. J. Lucassen, A. Salehi, & R. M. Buijs (Eds.), *Handbook of clinical neurology* (pp. 385–402). Elsevier.
- Harris, N. A., Isaac, A. T., Günther, A., Merkel, K., Melchior, J., Xu, M., Eguakun, E., Perez, R., Nabit, B. P., Flavin, S., Gilsbach, R., Shonesy, B., Hein, L., Abel, T., Baumann, A., Matthews, R., Centanni, S. W., & Winder, D. G. (2018). Dorsal BNST α 2A-adrenergic receptors produce HCN-dependent excitatory actions that initiate anxiogenic behaviors. *The Journal of Neuroscience*, 38(42), 8922–8942. <https://doi.org/10.1523/JNEUROSCI.0963-18.2018>
- Holstege, G., Meiners, L., & Tan, K. (1985). Projections of the bed nucleus of the stria terminalis to the mesencephalon, pons, and medulla oblongata in the cat. *Experimental Brain Research*, 58(2), 379–391. <https://doi.org/10.1007/BF00235319>
- Hwa, L. S., Neira, S., Pina, M. M., Pati, D., Calloway, R., & Kash, T. L. (2019). Predator odor increases avoidance and glutamatergic synaptic transmission in the prelimbic cortex via corticotropin-releasing factor receptor 1 signaling. *Neuropsychopharmacology*, 44(4), 766–775. <https://doi.org/10.1038/s41386-018-0279-2>
- Jansen, N. A., Schenke, M., Voskuyl, R. A., Thijs, R. D., van den Maagdenberg, A. M. J. M., & Tolner, E. A. (2019). Apnea associated with brainstem seizures in *Cacna1a*S218L mice is caused by medullary spreading depolarization. *The Journal of Neuroscience*, 39(48), 9633–9644. <https://doi.org/10.1523/JNEUROSCI.1713-19.2019>.
- Jefferys, J. G. R., Arafat, M. A., Irazoqui, P. P., & Lovick, T. A. (2019). Brainstem activity, apnea, and death during seizures induced by intrahippocampal kainic acid in anaesthetized rats. *Epilepsia*, 60(12), 2346–2358. <https://doi.org/10.1111/epi.16374>
- Johnson, M., Samudra, N., Gallagher, M. J., Abou-Khalil, B., & Nobis, W. P. (2021). Near SUDEP during bilateral stereo-EEG monitoring characterized by diffuse postictal EEG suppression. *Epilepsia*, 62(4), e60–e64. <https://doi.org/10.1111/epi.16852>.
- Kaur, S., Pedersen, N. P., Yokota, S., Hur, E. E., Fuller, P. M., Lazarus, M., Chamberlin, N. L., & Saper, C. B. (2013). Glutamatergic signaling from the parabrachial nucleus plays a critical role in hypercapnic arousal. *Journal of Neuroscience*, 33(18), 7627–7640. <https://doi.org/10.1523/JNEUROSCI.0173-13.2013>
- Kim, S.-R., & Kim, S.-Y. (2021). Functional dissection of glutamatergic and GABAergic neurons in the bed nucleus of the stria terminalis. *Molecules and Cells*, 44(2), 63–67. <https://doi.org/10.14348/molcells.2021.0006>
- Kim, S.-Y., Adhikari, A., Lee, S. Y., Marshel, J. H., Kim, C. K., Mallory, C. S., Lo, M., Pak, S., Mattis, J., Lim, B. K., Malenka, R. C., Warden, M. R., Neve, R., Tye, K. M., & Deisseroth, K. (2013). Diverging neural pathways assemble a behavioural state from separable features in anxiety. *Nature*, 496(7444), 219–223. <https://doi.org/10.1038/nature12018>
- Kodani, S., Soya, S., & Sakurai, T. (2017). Excitation of GABAergic neurons in the bed nucleus of the stria terminalis triggers immediate transition from non-rapid eye movement sleep to wakefulness in mice. *The Journal of Neuroscience*, 37(30), 7164–7176. <https://doi.org/10.1523/JNEUROSCI.0245-17.2017>
- Kommajosyula, S. P., & Faingold, C. L. (2019). Neural activity in the periaqueductal gray and other specific subcortical structures is enhanced when a selective serotonin reuptake inhibitor selectively prevents seizure-induced sudden death in the DBA/1 mouse model of sudden unexpected death in epilepsy. *Epilepsia*, 60(6), 1221–1233. <https://doi.org/10.1111/epi.14759>.
- Kommajosyula, S. P., Randall, M. E., Brozoski, T. J., Odintsov, B. M., & Faingold, C. L. (2017). Specific subcortical structures are activated during seizure-induced death in a model of sudden unexpected death in epilepsy (SUDEP): A manganese-enhanced magnetic resonance imaging study. *Epilepsy Research*, 135, 87–94. <https://doi.org/10.1016/j.eplepsyres.2017.05.011>
- Lacuey, N., Zonjy, B., Londono, L., & Lhatoo, S. D. (2017). Amygdala and hippocampus are symptomatogenic zones for central apneic seizures. *Neurology*, 88(7), 701–705. <https://doi.org/10.1212/WNL.0000000000003613>
- Lavezzi, A. M., Ferrero, S., Paradiso, B., Chamitava, L., Pisciolli, F., & Pusioli, T. (2019). Neuropathology of early sudden infant death syndrome-hypoplasia of the pontine kolliker-fuse nucleus: A possible marker of unexpected collapse during skin-to-skin care. *American Journal of Perinatology*, 36(05), 460–471. <https://doi.org/10.1055/s-0038-1669398>
- Lawlor, P. A., Bland, R. J., Mouravlev, A., Young, D., & During, M. J. (2009). Efficient gene delivery and selective transduction of glial cells in the mammalian brain by AAV serotypes isolated from nonhuman primates. *Molecular Therapy*, 17(10), 1692–1702. <https://doi.org/10.1038/mt.2009.170>
- Lebow, M. A., & Chen, A. (2016). Overshadowed by the amygdala: The bed nucleus of the stria terminalis emerges as key to psychiatric disorders. *Molecular Psychiatry*, 21, 450–463. <https://doi.org/10.1038/mp.2016.1>.
- Lertwittayanon, W., Devinsky, O., & Carlen, P. L. (2019). Cardiorespiratory depression from brainstem seizure activity in freely moving rats. *Neurobiology of Disease*, 134, 104628. <https://doi.org/10.1016/j.nbd.2019.104628>
- Li, M. M., Madara, J. C., Steger, J. S., Krashes, M. J., Balthasar, N., Campbell, J. N., Resch, J. M., Conley, N. J., Garfield, A. S., & Lowell, B. B. (2019). The paraventricular hypothalamus regulates satiety and prevents obesity via two genetically distinct circuits. *Neuron*, 102(3), 653–667.e6. <https://doi.org/10.1016/j.neuron.2019.02.028>
- Luskin, A. T., Bhatti, D. L., Mulvey, B., Pedersen, C. E., Girven, K. S., Oden-Brunson, H., Kimbell, K., Blackburn, T., Sawyer, A., Gereau IV, R. W., Dougherty, J. D., & Bruchas, M. R. (2021). Extended amygdala-parabrachial circuits alter threat assessment and regulate feeding. *Science Advances*, 7(9), eabd3666. <https://doi.org/10.1126/sciadv.abd3666>
- Marincovich, A., Bravo, E., Dlouhy, B., & Richerson, G. B. (2019). Amygdala lesions reduce seizure-induced respiratory arrest in DBA/1 mice. *Epilepsy & Behavior*, 121(Pt B), 106440. <https://doi.org/10.1016/j.yebeh.2019.07.041>
- Martin, B., Dieuset, G., Pawluski, J. L., Costet, N., & Biraben, A. (2020). Audiogenic seizure as a model of sudden death in epilepsy: A comparative study between four inbred mouse strains from early life to adulthood. *Epilepsia*, 61(2), 342–349. <https://doi.org/10.1111/epi.16432>

- Masneuf, S., Lowery-Gionta, E., Colacicco, G., Pleil, K. E., Li, C., Crowley, N., Flynn, S., Holmes, A., & Kash, T. (2014). Glutamatergic mechanisms associated with stress-induced amygdala excitability and anxiety-related behavior. *Neuropharmacology*, *85*, 190–197. <https://doi.org/10.1016/j.neuropharm.2014.04.015>
- Nobis, W. P., González Otárola, K. A., Templer, J. W., Gerard, E. E., VanHaerents, S., Lane, G., Zhou, G., Rosenow, J. M., Zelano, C., & Schuele, S. (2019). The effect of seizure spread to the amygdala on respiration and onset of ictal central apnea. *Journal of Neurosurgery*, *132*(5), 1313–1323. <https://doi.org/10.3171/2019.1.JNS183157>
- Nobis, W. P., Schuele, S., Templer, J. W., Zhou, G., Lane, G., Rosenow, J. M., & Zelano, C. (2018). Amygdala-stimulation-induced apnea is attention and nasal-breathing dependent. *Annals of Neurology*, *83*(3), 460–471. <https://doi.org/10.1002/ana.25178>
- Panneton, W. M., Gan, Q., Le, J., Livergood, R. S., Clerc, P., & Juric, R. (2012). Activation of brainstem neurons by underwater diving in the rat. *Frontiers in Physiology*, *3*, 111. <https://doi.org/10.3389/fphys.2012.00111>
- Partridge, J. G., Forcelli, P. A., Luo, R., Cashdan, J. M., Schulkin, J., Valentino, R. J., & Vicini, S. (2016). Stress increases GABAergic neurotransmission in CRF neurons of the central amygdala and bed nucleus stria Terminalis. *Neuropharmacology*, *107*, 239–250. <https://doi.org/10.1016/j.neuropharm.2016.03.029>
- Pollak Dorocic, I., Fürth, D., Xuan, Y., Johansson, Y., Pozzi, L., Silberberg, G., Carlén, M., & Meletis, K. (2014). A whole-brain atlas of inputs to serotonergic neurons of the dorsal and median raphe nuclei. *Neuron*, *83*(3), 663–678. <https://doi.org/10.1016/j.neuron.2014.07.002>
- Rhone, A. E., Kovach, C. K., Harmata, G. I., Sullivan, A. W., Tranel, D., Ciliberto, M. A., Howard, M. A., Richerson, G. B., Steinschneider, M., Wemmie, J. A., & Dlouhy, B. J. (2020). A human amygdala site that inhibits respiration and elicits apnea in pediatric epilepsy. *JCI Insight*, *5*(6), e134852. <https://doi.org/10.1172/jci.insight.134852>
- Ryvlin, P., Nashef, L., Lhatoo, S. D., Bateman, L. M., Bird, J., Bleasel, A., Boon, P., Crespel, A., Dworetzky, B. A., Høgenhaven, H., Lerche, H., Maillard, L., Malter, M. P., Marchal, C., Murthy, J. M., Nitsche, M., Pataria, E., Rabben, T., Rheims, S., & ... Tomson, T. (2013). Incidence and mechanisms of cardiorespiratory arrests in epilepsy monitoring units (MORTEMUS): A retrospective study. *The Lancet Neurology*, *12*(10), 966–977. [https://doi.org/10.1016/S1474-4422\(13\)70214-X](https://doi.org/10.1016/S1474-4422(13)70214-X)
- Schiavo, G., Benfenati, F., Poulain, B., Rossetto, O., Polverino de Laureto, P., DasGupta, B. R., & Montecucco, C. (1992). Tetanus and botulinum-B neurotoxins block neurotransmitter release by proteolytic cleavage of synaptobrevin. *Nature*, *359*(6398), 832–835. <https://doi.org/10.1038/359832a0>
- Schilling, W. P., McGrath, M. K., Yang, T., Glazebrook, P. A., Faingold, C. L., & Kunze, D. L. (2019). Simultaneous cardiac and respiratory inhibition during seizure precedes death in the DBA/1 audiogenic mouse model of SUDEP. *PLoS One*, *14*(10), e0223468. <https://doi.org/10.1371/journal.pone.0223468>
- Schoch, S., Deák, F., Königstorfer, A., Mozhayeva, M., Sara, Y., Südhof, T. C., & Kavalali, E. T. (2001). SNARE Function analyzed in synaptobrevin/VAMP knockout mice. *Science (New York, N.Y.)*, *294*(5544), 1117–1122. <https://doi.org/10.1126/science.1064335>
- Sveinsson, O., Andersson, T., Carlsson, S., & Tomson, T. (2017). The incidence of SUDEP. *Neurology*, *89*(2), 170–177. <https://doi.org/10.1212/WNL.0000000000004094>
- Taugher, R. J., Lu, Y., Wang, Y., Kreple, C. J., Ghobbeh, A., Fan, R., Sowers, L. P., & Wemmie, J. A. (2014). The bed nucleus of the stria Terminalis is critical for anxiety-related behavior evoked by CO₂ and acidosis. *Journal of Neuroscience*, *34*(31), 10247–10255. <https://doi.org/10.1523/JNEUROSCI.1680-14.2014>
- Tio, E., Culler, G. W., Bachman, E. M., & Schuele, S. (2020). Ictal central apneas in temporal lobe epilepsies. *Epilepsy & Behavior*, *112*, 107434. <https://doi.org/10.1016/j.yebeh.2020.107434>
- Torruella-Suárez, M. L., & McElligott, Z. A. (2020). Neurotensin in reward processes. *Neuropharmacology*, *167*, 108005. <https://doi.org/10.1016/j.neuropharm.2020.108005>
- Varga, A. G., Maletz, S. N., Bateman, J. T., Reid, B. T., & Levitt, E. S. (2020). Neurochemistry of the Kölliker-Fuse nucleus from a respiratory perspective. *Journal of Neurochemistry*, *156*(1), 16–37. <https://doi.org/10.1111/jnc.15041>
- Venit, E. L., Shepard, B. D., & Seyfried, T. N. (2004). Oxygenation prevents sudden death in seizure-prone mice. *Epilepsia*, *45*(8), 993–996. <https://doi.org/10.1111/j.0013-9580.2004.02304.x>
- Vilella, L., Lacuey, N., Hampson, J. P., Sandhya Rani, M. R., Sainju, R. K., Friedman, D., Nei, M., Strohl, K., Scott, C., Gehlbach, B. K., Zonjy, B., Hupp, N. J., Zaremba, A., Shafiabadi, N., Zhao, X., Reick-Mitrisin, V., Schuele, S., Ogren, J., Harper, R. M., & ... Lhatoo, S. D. (2018). Postconvulsive central apnea as a biomarker for sudden unexpected death in epilepsy (SUDEP). *Neurology*, *92*(3), e171–e182. <https://doi.org/10.1212/WNL.0000000000006785>
- Weissbourd, B., Ren, J., DeLoach, K. E., Guenther, C. J., Miyamichi, K., & Luo, L. (2014). Presynaptic partners of dorsal raphe serotonergic and GABAergic neurons. *Neuron*, *83*(3), 645–662. <https://doi.org/10.1016/j.neuron.2014.06.024>
- Yaguchi, M., Ohashi, Y., Tsubota, T., Sato, A., Koyano, K. W., Wang, N., & Miyashita, Y. (2013). Characterization of the properties of seven promoters in the motor cortex of rats and monkeys after lentiviral vector-mediated gene transfer. *Human Gene Therapy Methods*, *24*(6), 333–344. <https://doi.org/10.1089/hgtb.2012.238>
- Yamamoto, M., Wada, N., Kitabatake, Y., Watanabe, D., Anzai, M., Yokoyama, M., Teranishi, Y., & Nakanishi, S. (2003). Reversible suppression of glutamatergic neurotransmission of cerebellar granule cells in vivo by genetically manipulated expression of tetanus neurotoxin light chain. *The Journal of Neuroscience*, *23*(17), 6759–6767. <https://doi.org/10.1523/JNEUROSCI.23-17-06759.2003>
- Yan, W. W., Xia, M., Chiang, J., Levitt, A., Hawkins, N., Kearney, J., Swanson, G. T., Chetkovich, D., & Nobis, W. P. (2021). Enhanced synaptic transmission in the extended amygdala and altered excitability in an extended amygdala to brainstem circuit in a Dravet syndrome mouse model. *eNeuro*, *8*(3), ENEURO.0306–20.2021. <https://doi.org/10.1523/ENEURO.0306-20.2021>
- Zeng, C., Long, X., Cotten, J. F., Forman, S. A., Solt, K., Faingold, C. L., & Feng, H.-J. (2015). Fluoxetine prevents respiratory arrest without enhancing ventilation in DBA/1 mice. *Epilepsy & Behavior*, *45*, 1–7. <https://doi.org/10.1016/j.yebeh.2015.02.013>
- Zhang, H., Zhao, H., & Feng, H.-J. (2017). Atomoxetine, a norepinephrine reuptake inhibitor, reduces seizure-induced respiratory

- arrest. *Epilepsy & Behavior*, 73, 6–9. <https://doi.org/10.1016/j.yebeh.2017.04.046>
- Zhang, H., Zhao, H., Zeng, C., Van Dort, C., Faingold, C. L., Taylor, N. E., Solt, K., & Feng, H.-J. (2018). Optogenetic activation of 5-HT neurons in the dorsal raphe suppresses seizure-induced respiratory arrest and produces anticonvulsant effect in the DBA/1 mouse SUDEP model. *Neurobiology of Disease*, 110, 47–58. <https://doi.org/10.1016/j.nbd.2017.11.003>
- Zhang, R., Tan, Z., Niu, J., & Feng, H.-J. (2021). Adrenergic $\alpha 2$ receptors are implicated in seizure-induced respiratory arrest in DBA/1 mice. *Life Sciences*, 284, 119912. <https://doi.org/10.1016/j.lfs.2021.119912>
- Zingg, B., Peng, B., Huang, J., Tao, H. W., & Zhang, L. I. (2020). Synaptic specificity and application of anterograde transsynaptic AAV for probing neural circuitry. *The Journal of Neuroscience*, 40(16), 3250–3267. <https://doi.org/10.1523/JNEUROSCI.2158-19.2020>